# EXPERIMENTAL AND SIMULATION STUDY OF PLASMA DETACHMENT IN THE LINEAR PLASMA DEVICE MPS-LD

Chaofeng Sang*
School of Physics, Dalian University of Technology
Dalian, China
Email: sang@dlut.edu.cn

Changjiang Sun, Jintao Wu, Yue Wang, Yao Peng, Hao Wang, Qi Wang, Dezhen Wang
School of Physics, Dalian University of Technology
Dalian, China

## Abstract

Plasma detachment is a commonly employed divertor operation regime that effectively reduces the plasma temperature and heat flux near the target. However, divertor physics involves highly complex processes, including plasma transport, atomic and molecular collisions, and plasma–wall interactions. Conducting such studies in tokamak devices is costly, experimentally challenging, and diagnostically demanding. Therefore, it is essential to create relevant conditions in laboratory settings to enable controlled investigations. In this work, plasma detachment was studied by MPS-LD experiment and corresponding numerical simulations. Hydrogen discharge experiments were carried out, in which electron density and ion temperature were controlled by scanning discharge power and ion heating power. Upstream plasma density and temperature were measured using probes and Thomson scattering, while plasma parameters and deposited heat flux at the target plate were obtained with probes, and infrared camera. Spectroscopic diagnostics further provided insights into collision processes and ion composition. On this basis, numerical simulations were performed using SOLPS-ITER and BOUT++. The dependence of the main plasma parameters on the discharge parameters were obtained. The plasma detachment was achieved by injecting hydrogen in the target region. The impact of biasing on the plasma transport was also studied, revealing the variation of $n_e$ and $T_e$ with the varying bias value.

## 1. INTRODUCTION

The detached divertor operation regime is beneficial for reducing the target heat load and erosion rate in future magnetic confinement fusion reactors [1], and it is essential to conduct in-depth investigations into the associated physical collisional processes and the underlying mechanisms. However, in tokamak experiments, isolating the effect of a single parameter is challenging, and diagnostics are also difficult, limiting our understanding of detachment. The accuracy of numerical models heavily depends on validation with experimental data, and discrepancies exist between tokamak experiments and simulations in addressing key issues such as energy radiation [2]. Therefore, there is an urgent need to create relevant conditions in laboratory settings and conduct experimental studies. Linear plasma devices generate high-density plasmas using plasma sources and confine them with magnetic fields to form intense plasma beams, providing an excellent platform for studying tokamak divertor plasmas. The Multiple Plasma Simulation Linear Device (MPS-LD) [3], which is a newly constructed large linear device at Dalian University of Technology in China, aiming at studying the edge plasma of tokamak, offers new opportunities for in-depth studies of plasma detachment.

In this work, the recent progress of the MPS-LD device in detachment investigation is reported. First, steady-state hydrogen plasma discharges are achieved in the MPS-LD using a helicon plasma source, and the variations of $n_e$ and $T_e$ with magnetic field strength and gas flow rate are studied. The optimal discharge parameters are obtained. Subsequently, edge plasma code SOLPS-ITER and BOUT++ are employed to investigate hydrogen plasma transport and detachment in the MPS-LD device. By increasing the neutral gas pressure in the target chamber where the plasma interacts with the target material, reductions in plasma pressure and the heat flux delivered to the target are observed with increasing gas pressure, ultimately leading to plasma detachment. The impact of target bias on the target plasma parameters is obtained.

The paper is organized as follows. In section 2, the MPS-LD device along with its diagnostic systems and simulation setup are introduced. Section 3 presents the experimental and simulation results of hydrogen helicon discharge characteristics and detachment studies. In MPS-LD device, hydrogen helicon discharge experiments are carried out in combination with numerical simulations, and the hydrogen plasma transport and detachment are investigated, revealing the underlying roles of neutral gas injection and target biasing. Finally, the main conclusions are summarized and future work is discussed.

## 2. EXPERIMENTAL AND SIMULATION SETUP

### 2.1. Experimental setup

The vacuum of MPS-LD device consists of four regions: the plasma source region, heating region, target region, and sample exchange region. The first three regions are 3 meters in length, with diameters of 0.4 meters, 0.4 meters, and 0.6 meters, respectively. MPS-LD is equipped with 11 conventional copper magnets, each independently powered, allowing flexible control of various magnetic field configurations by adjusting the current and magnet position. The maximum axial magnetic field strength is about 0.4 Tesla. MPS-LD utilizes a helicon plasma source to generate high-density plasma, with an RF power of 20 kW and a frequency of 13.56 MHz [4]. The device is also equipped with an ion cyclotron resonance heating (ICRH) system, operating at a RF power of 10 kW and a frequency of 0.9 MHz [5]. FIG. 1 shows a photograph of MPS-LS device and a typical discharge image.

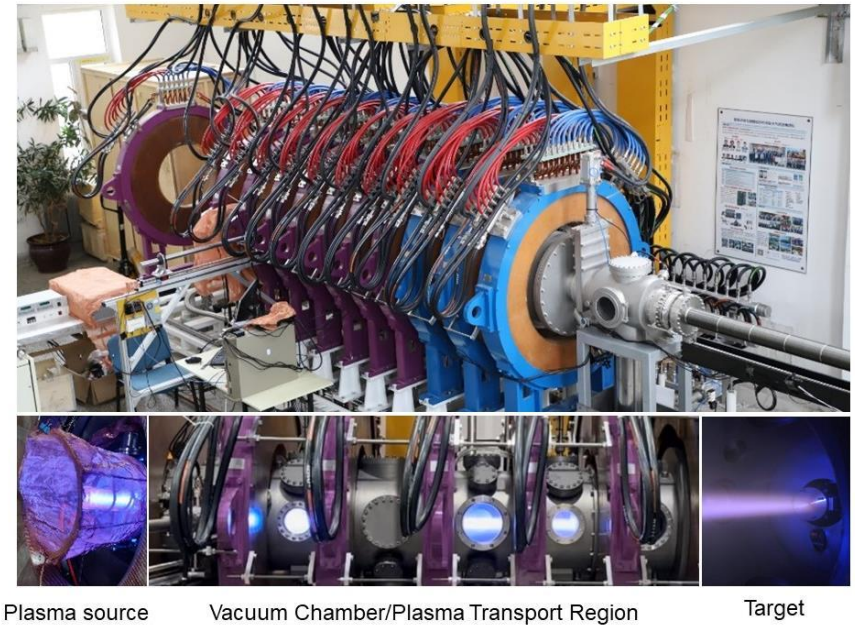


*FIG. 1. MPS-LD device and typical plasma discharge image.*

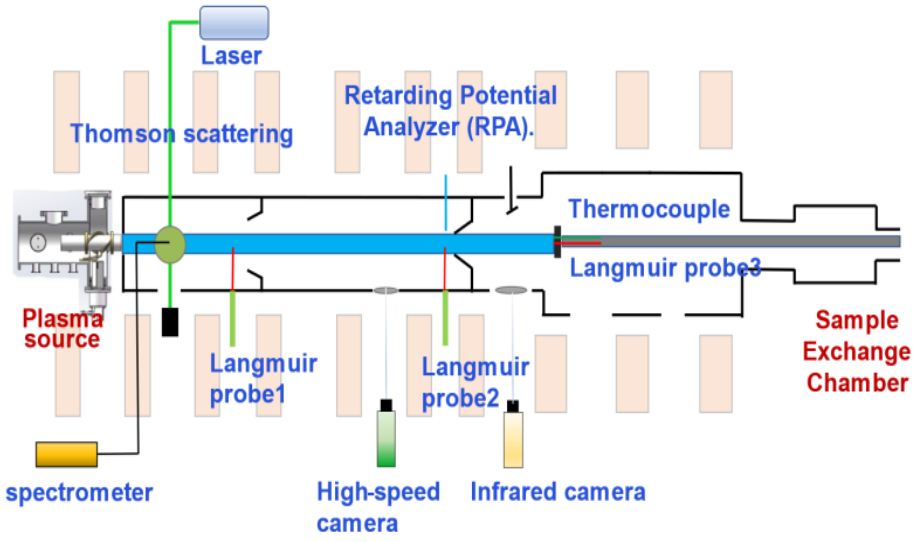


*FIG. 2. Diagram of the diagnostic system in MPS-LD device.*

A variety of diagnostic systems have been developed for MPS-LD, as shown in FIG. 2. It includes three sets of Langmuir probes, a Thomson scattering system, a spectrometer, a retarding potential analyzer (RPA), an infrared camera, a high-speed camera, and thermocouples. These are used to measure basic parameters such as electron temperature, electron density, ion temperature, the heat flux of the target plate, and ion composition, providing data for experimental analysis and comparison with numerical simulations. MPS-LD device has conducted plasma discharges using various gases, including argon, helium, and hydrogen. This work primarily focuses on the experimental and simulation study of plasma detachment.

2.2. SOLPS-ITER simulation setup

SOLPS-ITER, which consists of the multi-fluid plasma transport code B2.5 [6] and the kinetic Monte Carlo neutral transport code EIRENE [7], has been applied to predict hydrogen (H) plasma transport in MPS-LD [8]. In this work, SOLPS-ITER is employed to simulate H plasma transport to understand the detachment mechanism.

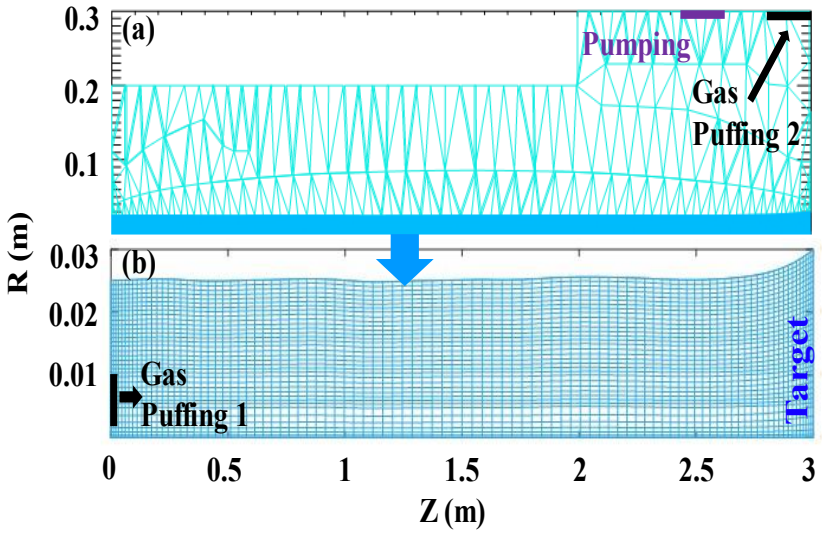


*FIG. 3. (a) The simulation mesh used in SOLPS-ITER consists of triangular meshes for neutral particle transport and quasi-orthogonal meshes for plasma transport. (b) Enlarged view of the quasi-orthogonal mesh.*

In the SOLPS simulations, the numerical meshes are generated according to the magnetic field and vacuum chamber structure. The simulations include only hydrogen ions, hydrogen atoms, and hydrogen molecules, and plasma–wall interactions occur only at the target. As shown in FIG. 3, working gas is injected through gas puffing 1 (GP1) to produce plasma, while additional neutrals are introduced into the target region through gas puffing 2 (GP2) to increase the neutral pressure and achieve plasma detachment. The recycling coefficient at the pumping location is set to $R$ = 0.95, corresponding to a pumping speed of 1.8 $m^3s^{-1}$. The boundary conditions are defined as follows: on the symmetry axis boundary, radial particle, energy, and momentum fluxes are set to zero; sheath conditions are imposed at both the plasma source and target boundaries; at the lateral wall boundary, decay length boundaries for density, temperature, and potential are enforced with prescribed values. During the simulations, the radial particle diffusion coefficients, electron and ion heat diffusivity coefficients, and recycling coefficients are treated as free variables and are adjusted according to the experiments.

2.3. BOUT++ simulation setup

An LPD module within the BOUT++ framework is developed for simulating plasmas in linear plasma devices, with an upgraded neutral module, which can handle more plasma-neutral collisions and recycling. The simulation results have been benchmarked against experimental measurements and SOLPS simulations, showing good overall agreement [9,10]. Moreover, a potential model was newly developed based on the LPD module, enabling self-consistent simulations of plasma transport under target biasing. BOUT++ LPD provides a fast, efficient, and accurate tool for modeling linear devices.

In the BOUT++ LPD setup, first the magnetic field configuration is calculated using the Linear Device Magnetic-field Configuration Calculation (LD-MCC) code, which outputs $A_\varphi$, $\psi$, and $B$. A standard interface is provided to

store these data together with the coordinates. Then, the magnetic field data is directly read by BOUT++ to generate the simulation mesh. The grid is aligned along magnetic field lines and resolved in both the axial (z) direction and the radial (r) direction perpendicular to the field lines. FIG. 4 illustrates the simplified schematic of the device and its corresponding simulation mesh. A non-uniform mesh is employed, with higher resolution allocated to the target region and along the axis, where detailed plasma behaviour is of particular focus. Boundary conditions can be found in Refs.[9, 10].

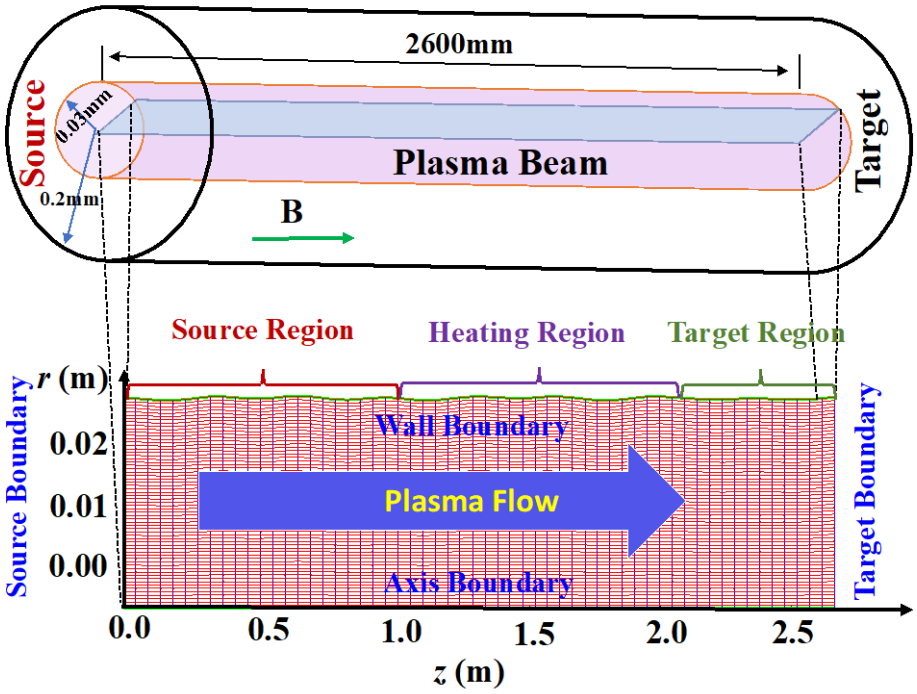


*FIG. 4. Simplified schematic of the MPS-LD device and the corresponding simulation mesh. The simulation domain shows the cross-section of the plasma column. The right boundary of the mesh corresponds to the target plate, the left boundary to the plasma source, the bottom boundary to the axis, and the top boundary to the vacuum wall, respectively*

## 3. RESULTS AND DISCUSSIONS

### 3.1. Hydrogen plasma discharge characteristics

In this work, hydrogen plasma discharge experiments are first carried out under a uniform magnetic field configuration to investigate the discharge characteristics and to determine the experimental conditions suitable for plasma detachment studies. In the experiment, we mainly used two sets of probes located in the source and the target region for diagnostics, in order to determine how the electron density in these two regions varies with the main parameters, as well as the differences in key parameters between the source and target regions. The plasma source power was fixed at 8000 W, and the electron density variation was first investigated by changing the magnetic field strength and the hydrogen gas flow rate.

FIG. 5(a) shows the evolution of $n_e$ in both the source and target regions as a function of magnetic field strength, while the hydrogen gas flow rate is fixed to 150 sccm. It can be observed that with increasing $B$, $n_e$ in both regions first increases and then decreases. In both regions, there exists an optimal magnetic field strength at which the electron density reaches its maximum. However, the optimal magnetic field strength corresponding to the maximum $n_e$ is lower in the target region (~150 Gs) than in the source region (200 Gs). This leads to the following results: when $B < 175$ G, $n_e$ is nearly uniformly distributed between the source and target regions, in this case, the $n_e$ in the target region is highest; when 175 G $< B <$ 250 G, $n_e$ in the source region is nearly two to three times that in the target region; and when $B > 250$ G, $n_e$ in the two regions becomes equal again but both decrease to their lowest values.

The optimal magnetic field in the target region ($B$ = 150 Gs) is chosen for further investigation. With the magnetic field strength fixed, only the hydrogen gas flow rate is varied. FIG. 5(b) presents the evolution of $n_e$ in the source and target regions as a function of gas flow rate. It can be observed that with increasing $fr$, $n_e$ in both regions first increases and then decreases, and the optimal $fr$ value corresponding to the maximum $n_e$ is higher in the target region than in the source region. This is mainly due to the combined effect of the influence of the gas flow rate on the helicon wave damping and the axial $n_e$ gradient [4].

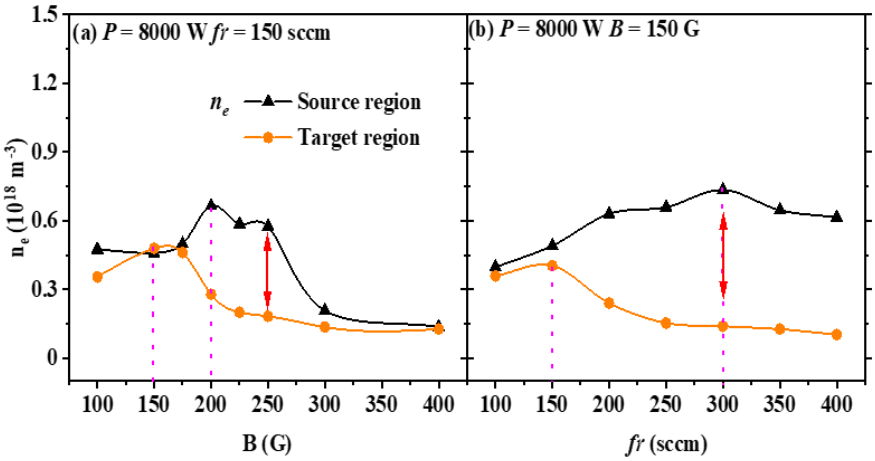


*FIG. 5. (a) The variations of ne on axis of (a) LP1 and LP2 with B from 100 ~ 400 G when fr = 150 sccm, (b) LP1 and LP2 with fr from 100 ~ 400 sccm when B = 150 G. The main parameters are P = 8000 W.*

Since the plasma parameters in the target region remain relatively low under the above experimental conditions, we further enhance the plasma density by employing a magnetic mirror configuration [11]. The effects of the magnetic mirror configurations are investigated. In the experiment, the magnetic field strength in the source region is kept at 150 G, and the magnetic field strength in the target region is increased to 800 G to construct a magnetic mirror configuration, as shown in FIG. 6(a). FIG. 6(b) shows the corresponding plasma density in the source and target region under this magnetic configuration. It can be observed that compared with the source region, $n_e$ in the target region under the magnetic mirror configuration decreases at the radial boundary and increases at the center of the plasma, i.e. $n_e \sim 1 \times 10^{18}$ m$^{-3}$ (mirror configuration) vs $n_e \sim 5 \times 10^{17}$ m$^{-3}$ (uniform magnetic field configuration, as shown in figure 4). This enhancement is attributed to the increased magnetic field strength in the target region, which leads to stronger helicon wave energy deposition and a radial concentration of plasma distribution. Since the magnetic mirror structure also causes the reflection of helicon wave, the $n_e$ in the source region will also increase to a certain extent compared with the uniform magnetic. FIG. 6(c) shows the corresponding electron temperature in both regions. It can be observed that $T_e$ in the two regions is not significantly changed at the center of plasma beam, both being around 3 to 6 eV. On the radial boundary of the plasma beam, $T_e$ is significantly higher in the target region than in the source region.

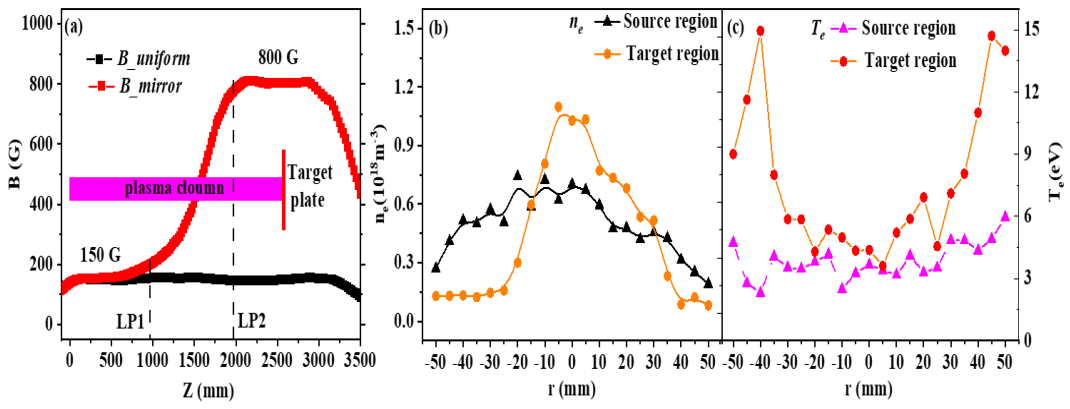

*FIG. 6. (a) The typical magnetic field configuration used in the experiment (along the axis); The radial profiles of (b) $n_e$ and (c) $T_e$ at LP1 and LP2 obtained from experiment at the B_mirror magnetic field configuration. The main parameters are B = 150 + 800 G, fr = 150 sccm and P = 8000 W.*

### 3.2. Simulation study of plasma detachment using SOLPS-ITER

Based on the experiment, a preliminary study on plasma detachment is carried out using SOLPS-ITER. First, the simulations are performed with the plasma source power fixed at 8 kW, hydrogen gas flow rate *fr* at GP1 set to 300 sccm, and a uniform magnetic field of 150 G. Under these discharge conditions, GP2 is then activated to inject hydrogen molecules at rates of $3 \times 10^{20}$ $H_2$ $s^{-1}$ and $5 \times 10^{20}$ $H_2$ $s^{-1}$, respectively, in order to study the variation of the neutral pressure ($P_{nt}$) in the target region and to evaluate its effects on the electron density ($n_{es}$) in the plasma source region as well as on the electron density ($n_{et}$) and particle flux ($\Gamma_t$) at the target.

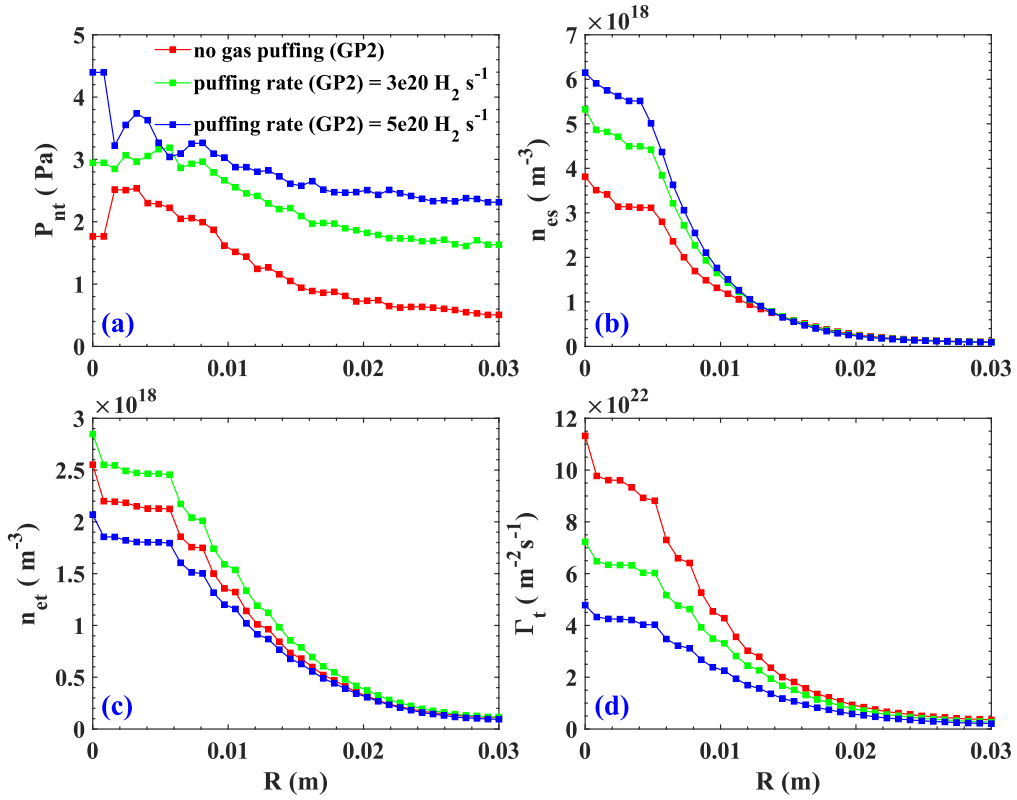


*FIG. 7. (a) The radial profiles of (a) $P_{nt}$, (b) $n_{es}$, (c) $n_{et}$, and (d) $\Gamma_t$ under different gas puffing rates at GP2.*

As shown in FIG. 7(a), with the increase of the gas puffing rate at GP2, $P_{nt}$ gradually rises from about 1 Pa to above 4 Pa near the target, resulting in the enhanced momentum and energy losses. In this process, as shown in FIG. 7(b), electron density in the source region $n_{es}$ exhibits a monotonically increasing trend, due to more ionization. Whereas, due to enhanced collisions, the ionization rate decreases with the reduction of electron temperature, resulting in a decrease of $n_{et}$ and $\Gamma_t$, accompanied by a reversal phenomenon, as shown in FIG. 7(c) and 7(d). It clearly indicates that the plasma detachment is achieved and the neutral particles plays significant role on the detachment process. It should be noted that both increased upstream density and direct injected neutral particles promote the achievement of the detachment.

### 3.3. Simulate the Influence of Biasing on plasma at the Target Using BOUT++LPD

In linear devices, variations in plasma parameters at the target plate are crucial for investigations into plasma transport and detachment. Therefore, we also investigated the effects of negative bias voltage ($U_{bias}$) on the electron density at the target ($n_{e,T}$) and electron temperature at the target ($T_{e,T}$) using the BOUT++ LPD module. Based on existing investigation results, the radial distribution of the plasma source in experiments typically follows a Gaussian profile. Accordingly, in the BOUT++ LPD module, we assumed that both the density and

temperature at the plasma source boundary obey a radial Gaussian distribution. Their peak values were set as follows: $n_{e,S}$ = 2.8×10$^{18}$ m$^{-3}$ and $T_{e,S}$ =21.0 eV. Considering the magnetic field strength of the discharge (0.15 T), the radial transport coefficients were set to $D_\perp$ = 0.4 m$^2$s$^{-1}$ and $\chi_{\perp i,e}$ = 0.75 m$^2$s$^{-1}$. The simulations conducted in this study include two cases: unbiased conditions ($U_{bias}$ = 0 V) and various negative bias voltages ($U_{bias}$ = −10 V、−40 V、−80 V、−120 V、−160 V、−200 V), as shown in FIG. 8.

After applying the negative bias voltage, see FIG. 8. In the range (− 40 V ≤ $U_{bias}$ < 0 V), with an increase in the absolute value of the bias voltage |$U_{bias}$|, $n_{e,T}$ decreases continuously, and $T_{e,T}$ also exhibits a decreasing trend, albeit with a smaller magnitude. In the range (− 200 V ≤ $U_{bias}$ < − 40 V), as |$U_{bias}$| increases, $T_{e,T}$ first reverses its trend and then increases significantly. In contrast, $n_{e,T}$ continues to decrease, and its variation amplitude is extremely small within the sub-range of − 200 V ≤ $U_{bias}$ ≤ −120 V. The reason can be attributed to the variation in ion velocity (with the flux remaining unchanged) and the energy gain through the work of the friction force. It should be noted that the power is actually supplied by the biasing source.

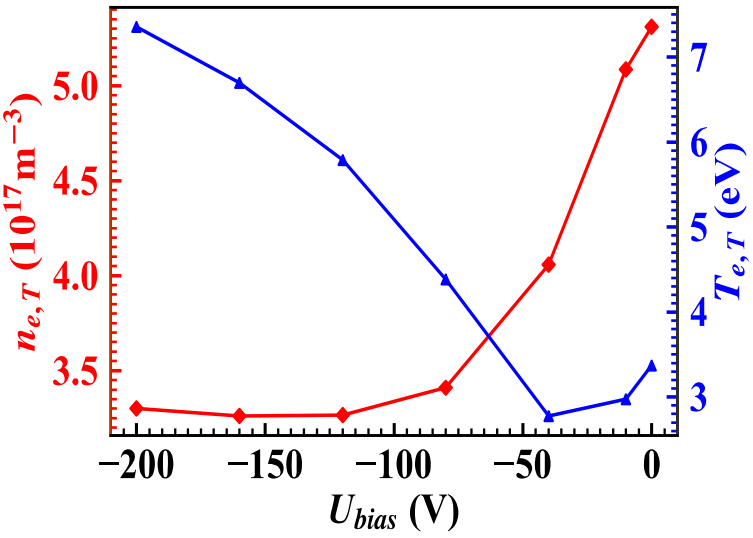


*FIG. 8. Simulated electron density $n_{e,T}$ and electron temperature $T_{e,T}$ at the target as functions of bias voltage $U_{bias}$.*

## 4. CONCLUSIONS

In this work, the hydrogen plasma transport and the detachment mechanism are investigated through experiments as well as SOLPS-ITER and BOUT++ simulations. The main results are as follows:

- The dependence of electron density on magnetic field strength and gas flow rate is investigated. For hydrogen discharges, there exists an optimal uniform magnetic field strength at which the electron density reaches its maximum—approximately 150 Gs in the target region and 200 Gs in the source region. The optimal gas flow rate for achieving a high electron density in the target region is 150 sccm. Furthermore, adopting a mirror magnetic field configuration can further enhance the electron density in the target region.
- Using SOLPS-ITER, the effect of hydrogen injection at the target region on plasma detachment in MPS-LD is investigated. The results show that neutral particle injection at the target region can effectively increase the neutral pressure, thereby achieving plasma detachment and particle flux reversal. The reason can be attributed to the enhanced collisional processes that lead to efficient energy dissipation.
- Using the BOUT++ LPD module, the effect of target biasing on plasma transport in MPS-LD is investigated. It is found that applying a bias voltage greater than 40 V effectively increases the electron temperature at the target, but simultaneously reduces the electron density. The reason can be attributed to the variation in ion velocity and the energy gain through the work of the friction force.

**ACKNOWLEDGEMENTS**

This work is supported by National Key R&D Program of China No.2024YFE03160000 and National Natural Science Foundation of China under Grant No. U2441223.

## REFERENCES


[1] Krasheninnikov S I, Kukushkin A S, Pshenov A A, 2016 Divertor plasma detachment Phys. Plasmas 23 055602.

[2] Canik J M, Briesemeister A R, McLean A G, 2017 Testing the role of molecular physics in dissipative divertor operations through helium plasmas at DIII-D Phys. Plasmas 24 056116.

[3] Sun C, Sang C, Ye H, 2021 The design of Multiple Plasma Simulation Linear Device Fusion Eng. Des. 162 112074.

[4] Wu J, Sang C, Sun C, 2024 Experimental and simulation study of argon helicon discharge in multiple plasma simulation linear device (MPS-LD) Plasma Sources Sci. Technol. 33 085007.

[5] Sun C, Zhang Y, Sang C, 2025 Experimental and simulation study of helium plasma transport during ion cyclotron resonance heating in MPS-LD Nucl. Fusion 65 056007.

[6] Schneider R, Bonnin X, Borrass K, 2006 Plasma Edge Physics with B2-Eirene Contrib. to Plasma Phys. 46 3–191.

[7] Reiter D, Baelmans M, Börner P, 2005 The EIRENE and B2-EIRENE Codes Fusion Sci. Technol. 47 172–186.

[8] Zhang Y, Sang C, Sun C, 2022 Simulation of plasma transport in the linear plasma device MPS-LD by SOLPS-ITER Nucl. Mater. Energy 33 101280.

[9] Wang Y, Sang C, Li N, 2022 Simulation of plasma transport in MPS-LD linear plasma device by using BOUT++ Plasma Phys. Control. Fusion 64 115010.

[10] Wang Y, Sun C, Sang C, 2024 Simulation ofthe impact of particle recycling on the plasma in MPS-LD device based on the BOUT++ LPD module *Contrib. to Plasma Phys.* **64** e202300132.

[11] Piotrowicz P A, Caneses J F, Green D L, 2018 Helicon normal modes in Proto-MPEX *Plasma Sources Sci. Technol.* **27** 055016.